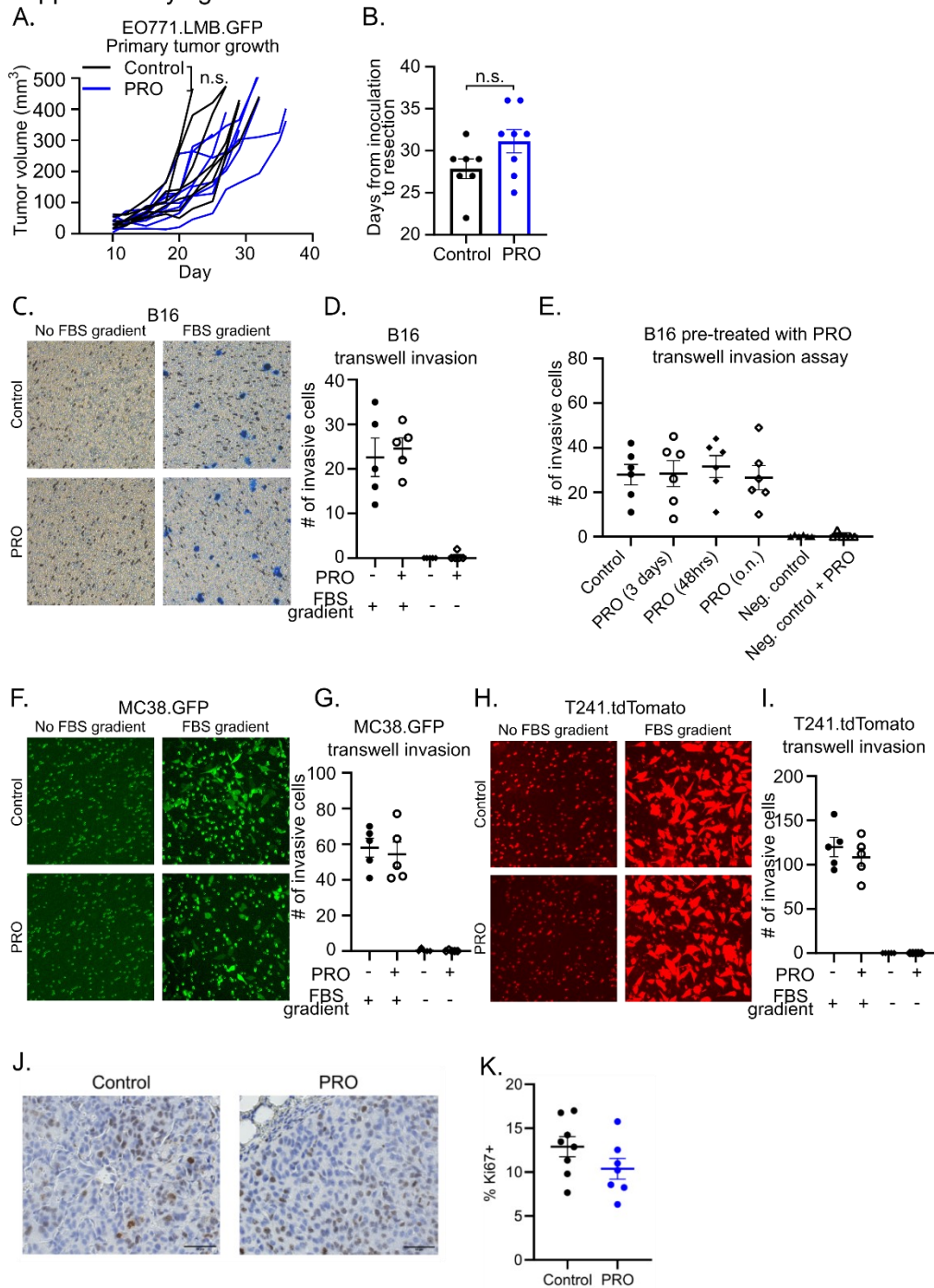
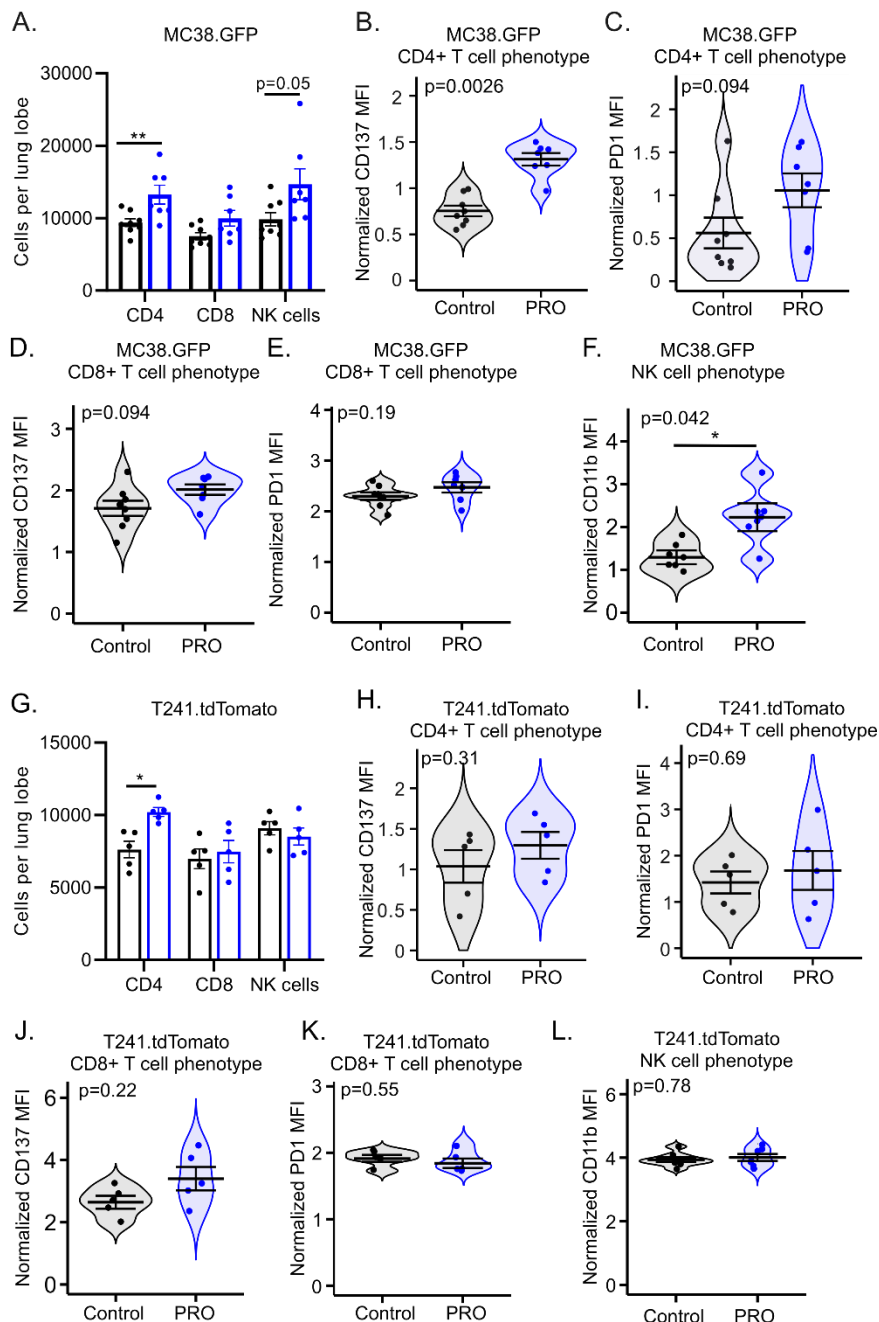


Supplementary figure 1.



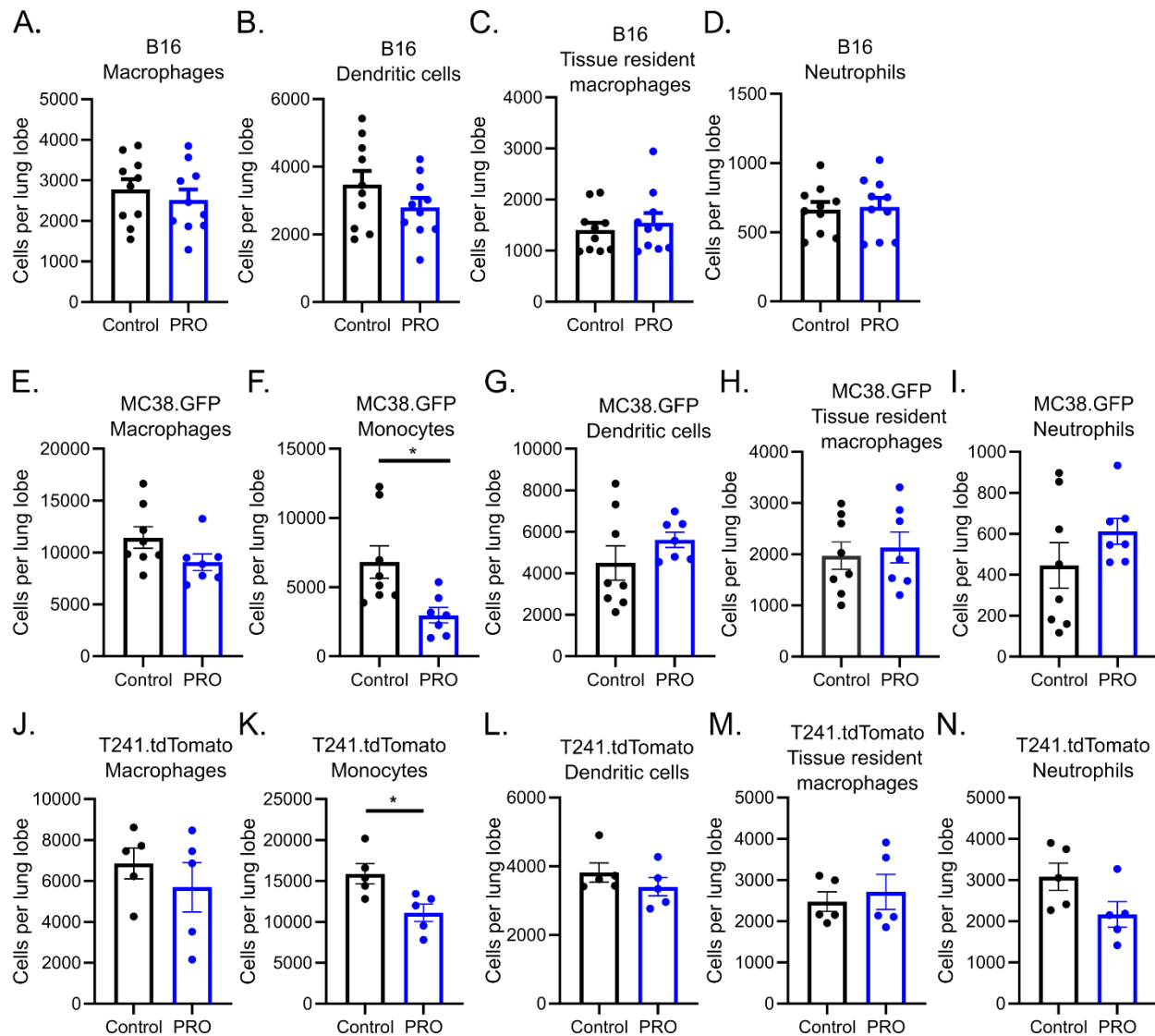
Supplementary figure S1. (A) Primary tumor growth of orthotopically inoculated EO771.LMB tumors. (B) Days from EO771.LMB cell inoculation to surgical resection of primary tumors. (C-D) Representative transwell invasion experiment images (C) and quantification (D) of invasive B16 cells in the presence of propranolol (PRO). (E) Quantification of invasive B16 cells pretreated with PRO. (F-G) Representative transwell invasion experiment images (F) and quantification (G) of invasive MC38.GFP cells in the presence of PRO. (H-I) Representative transwell invasion experiment images (H) and quantification (I) of invasive T241.tdTomato cells in the presence of propranolol. (J-K) Representative Ki67 immunohistochemical staining (J) and quantification of Ki67 (K) in paraffin embedded metastasis bearing lung sections. n.s. not significant, according to TumGrowth software for tumor growth curves, or multiple t test with Bonferroni correction. Means \pm SEM are depicted.

Supplementary figure 2.



Supplementary figure S2. Flow cytometry was performed on single-cell suspension derived from either MC38 metastasis bearing lungs (A-F) or T241 metastasis bearing lungs (G-L). (A) Quantification of lung infiltrating CD4+, CD8+ and NK cells in MC38 metastasis bearing lungs. (B-C) Mean fluorescence intensity of CD137 (B) and PD1 (C) on CD4+ T cells in MC38 metastasis bearing lungs. (D-E) Mean fluorescence intensity of CD137 (D) and PD1 (E) on CD8+ T cells in MC38 metastasis bearing lungs. (F) Mean fluorescence intensity of CD11b on NK cells in MC38 metastasis bearing lungs. (G) Quantification of lung infiltrating CD4+, CD8+ and NK cells in T241 metastasis bearing lungs. (H-I) Mean fluorescence intensity of CD137 (H) and PD1 (I) on CD4+ T cells in T241 metastasis bearing lungs. (J-K) Mean fluorescence intensity of CD137 (J) and PD1 (K) on CD8+ T cells in T241 metastasis bearing lungs. (L) Mean fluorescence intensity of CD11b on NK cells in T241.tdTomato metastasis bearing lungs. (A-L) Each dot in the dot plots represents one mouse. *p < 0.05, **p < 0.01, according to multiple t test with Bonferroni correction. Mean \pm SEM are depicted.

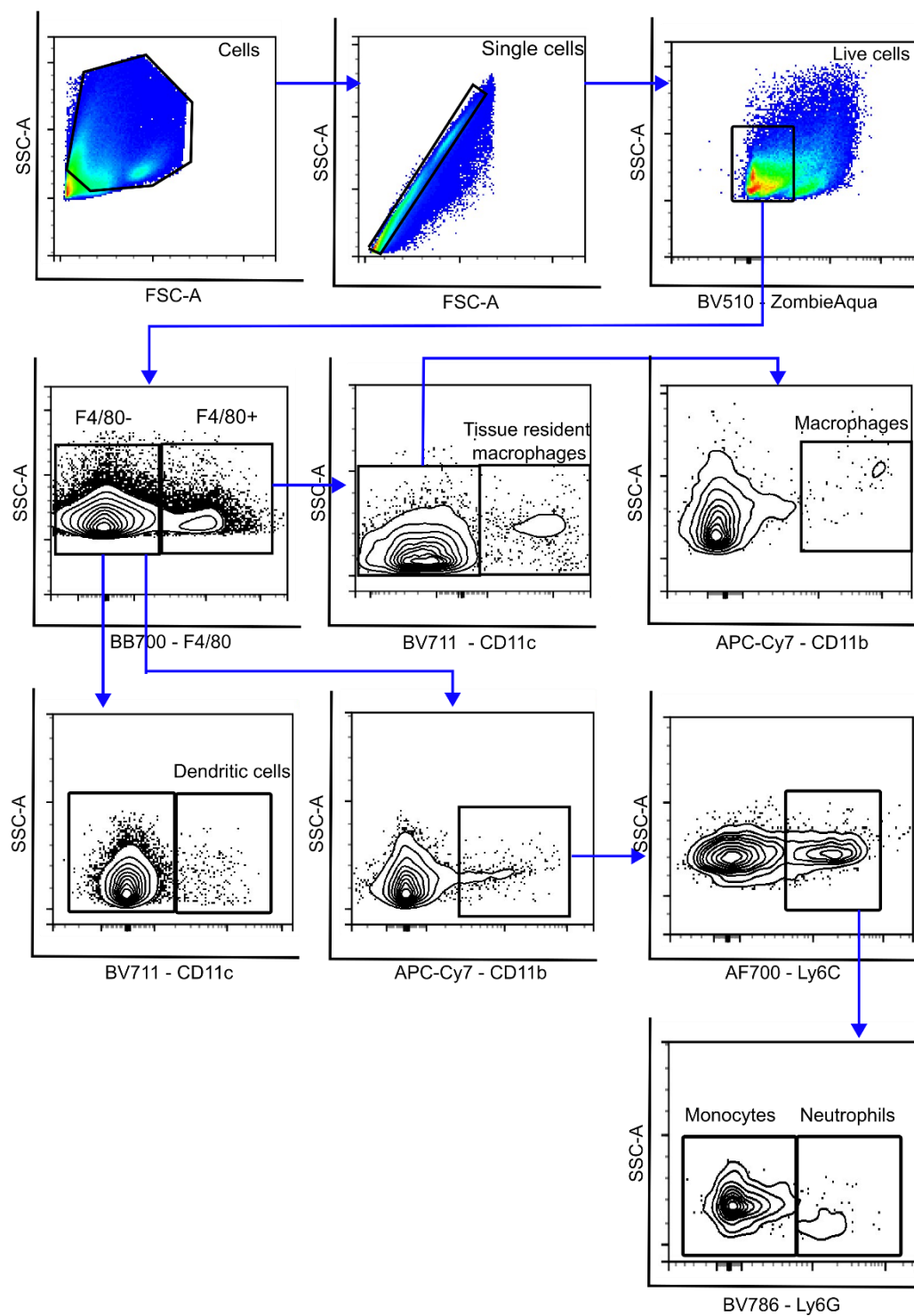
Supplementary figure 3.



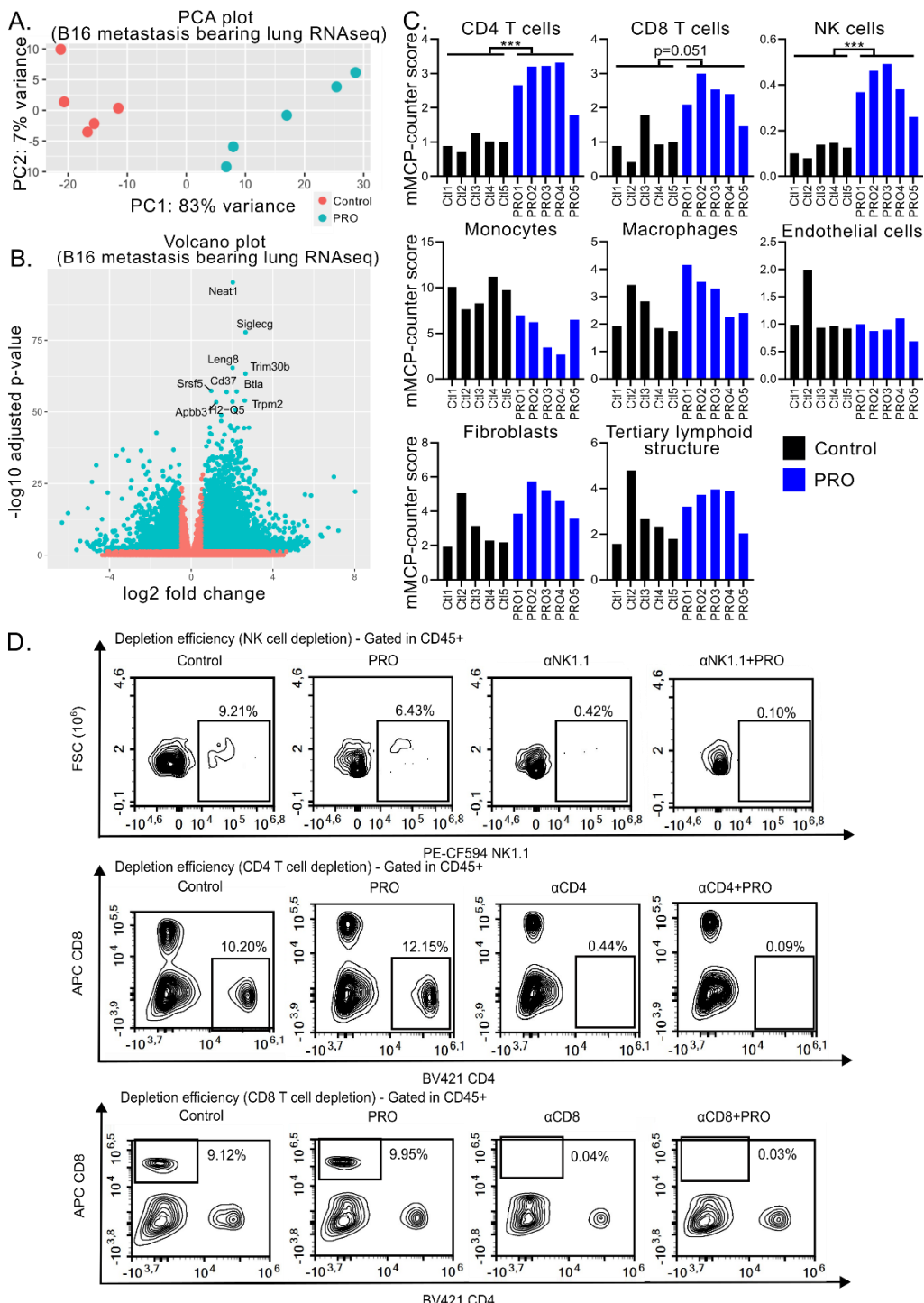
Supplementary figure S3. Flow cytometry was performed on single-cell suspension derived from B16, MC38 or T241 metastasis bearing lungs. For gating strategy, see supplementary figure S4. Quantification of macrophages in B16 (A), MC38 (E), or T241 (J) metastasis bearing lungs. Quantification of monocytes in MC38 (F), or T241 (K) metastasis bearing lungs. Quantification of dendritic cells in B16 (B), MC38 (G), or T241 (L) metastasis bearing lungs. Quantification of tissue resident macrophages in B16 (C), MC38 (H), or T241 (M) metastasis bearing lungs. Quantification of neutrophils in B16 (D), MC38 (I), or T241 (N) metastasis bearing lungs. (A-N) Each dot in the dot plots represents one mouse. * $p < 0.05$, according to multiple t test with Bonferroni correction. Means \pm SEM are depicted.

Supplementary figure 4.

A.

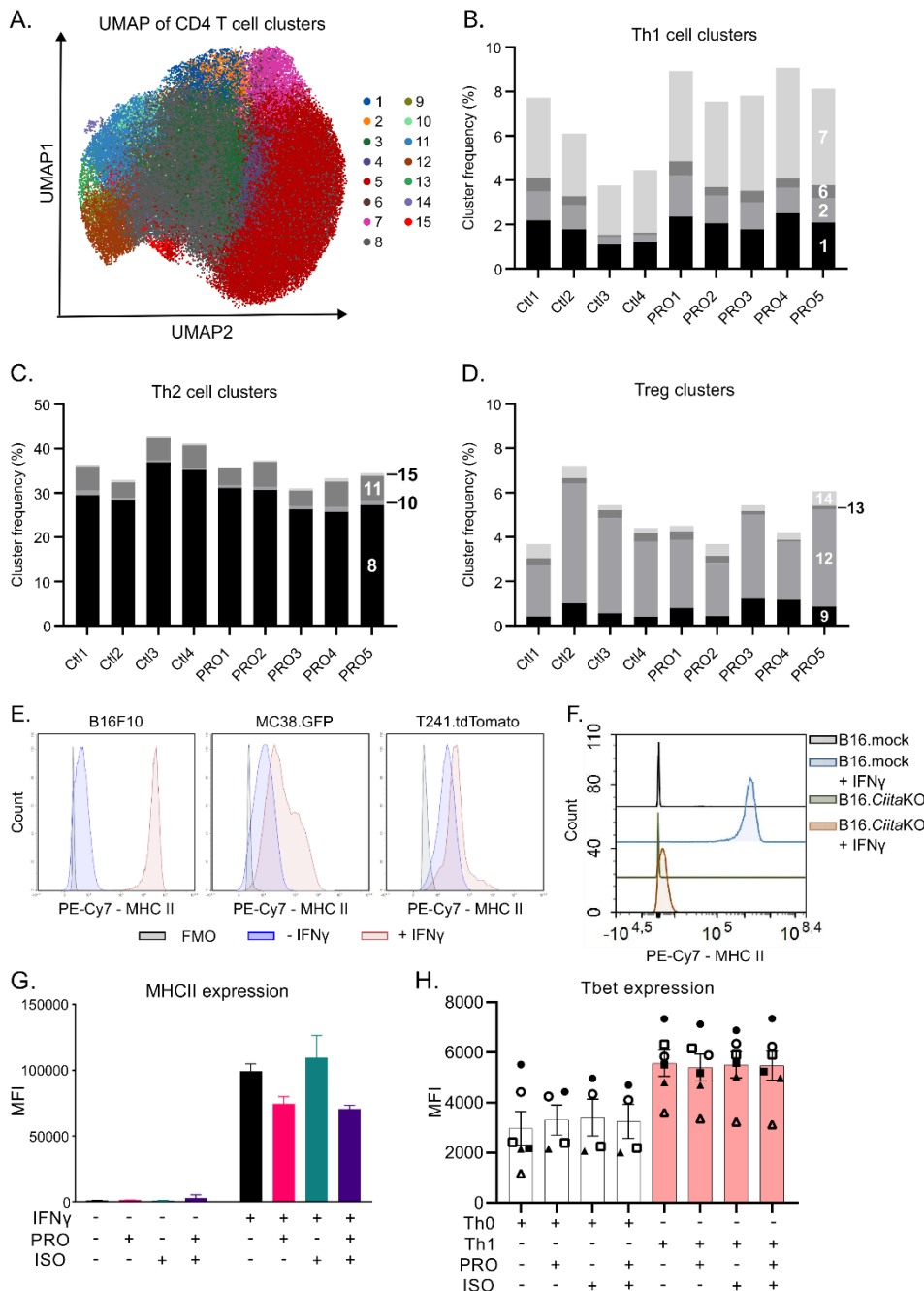


Supplementary figure 5.



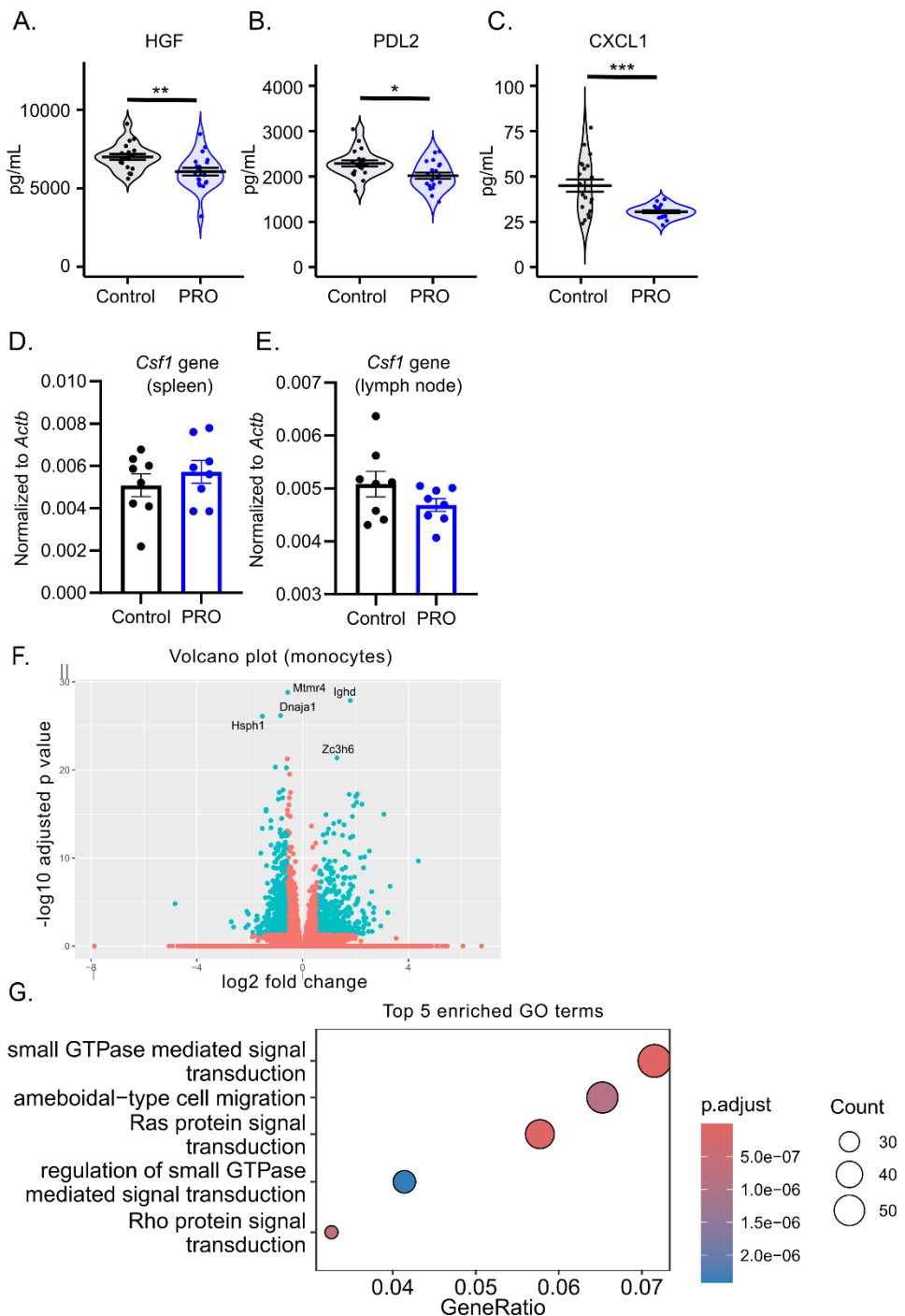
Supplementary figure S5. (A-C) RNA-seq analysis was performed on B16 metastasis bearing lungs on day 14 after cancer cell inoculation (n=5 per group). (A) Principal component analysis (PCA) plot of samples from control and PRO treated groups. (B) Volcano plot with highlight of top 10 upregulated genes in PRO treated group compared to control. (C) Murine Microenvironment Cell Population counter (mMCP) counter scores for immune cell populations in the metastasis bearing lungs based on the mMCP deconvolution tool. Each graph depicts a different population. (D) Flow cytometry-based confirmation of immune cell depletion in B16 metastasis bearing lungs from mice treated with antibodies for depletion of NK cells (top row), CD4+ T cells (middle row), or CD8+ T cells (bottom row).

Supplementary figure 6.



Supplementary figure S6. (A) UMAP distribution of relative expression (z score) of markers in unique CD4+ T cell FlowSOM clusters. (B-D) Lung infiltrating CD4+ T cells from control and PRO treated mice were isolated and stained for high dimensional flow cytometry clustering (n=5 per group). Stacked bar graphs depicting the cluster frequencies of Th1 clusters (B), Th2 clusters (C), and Treg clusters (D). (E) Flow cytometry quantification of MHC class II expression after 48 hours IFN γ stimulation on *in vitro* cultured B16, MC38, and T241 cells. (F) Flow cytometry quantification of MHC class II expression on *in vitro* cultured B16.mock and B16.CiitaKO cells with or without 48 hours IFN γ stimulation after FACS sorting. (G) MHC class II expression on B16 cells upon culture in the presence of isoprenaline, PRO, or both. (H) Human naive CD4+ T cells were isolated from healthy donors and polarized to Th0 or Th1 phenotypes in the presence of isoprenaline, PRO, or both, and intracellular mean fluorescence intensity (MFI) of Tbet expression was quantified by flow cytometry. Each symbol represents one donor and is an average of technical duplicates.

Supplementary figure 7.



Supplementary figure S7. (A-C) Olink proteomics analysis was performed on serum samples collected from control and PRO treated mice (n=20) on day 14. Absolute serum concentration of HGF (A), soluble PDL2 (B), and CXCL1 (C). qRT-PCR based quantification of *Csf1* gene expression in spleens (D) and lymph nodes (E) from B16 metastasis bearing mice. (F-G) RNA-seq analysis was performed on monocytes isolated from B16 metastasis bearing lungs from control and PRO treated mice on day 14 after cancer cell inoculation (n=4 per group). (F) Volcano plot with highlight of top 5 regulated genes in PRO treated group compared to control. (G) Top 5 enriched terms from gene ontology (GO) enrichment analysis of upregulated genes in PRO treated group compared to control. *p < 0.05, **p < 0.01, ***p < 0.005, according to multiple t test with Bonferroni correction. Means \pm SEM are depicted.